

Influence of resonant magnetic perturbations on plasma edge turbulence

R. M. Castro, M. V. A. P. Heller, I. L. Caldas,^{a)} Z. A. Brasília, R. P. da Silva,
and I. C. Nascimento

Institute of Physics, University of São Paulo, C. P. 66318, 05389-970 São Paulo, SP, Brazil

(Received 30 April 1996; accepted 30 September 1996)

This work reports alterations on plasma-edge equilibrium profiles and on edge turbulence, and anomalous transport induced by resonant perturbing magnetic fields in the TBR (Brazilian Tokamak) tokamak [J. Fusion Energy **12**, 295 (1993)]. Thus, these perturbations have reduced the equilibrium parameters and the spectral power of the fluctuations and enhanced their phase velocity. They have also reduced the particle flux at the plasma edge. All these electrostatic edge parameters have been computed by taking into account temperature fluctuation corrections. Although the perturbation slightly affected just the linear correlation between electrostatic fluctuations, its bispectral analysis shows a reduction of the quadratic mode coupling. Furthermore, the energy transferred between different spectral components, with and without the magnetic perturbation, did not have the same direction for all fluctuations. Finally, the normal probability distribution functions of the fluctuations show significant non-Gaussian features, although the fluctuating potential distribution became near Gaussian with the magnetic perturbation. © 1997 American Institute of Physics. [S1070-664X(97)01001-X]

I. INTRODUCTION

The interest in controlling plasma edge is based on the evidence that improvements of the plasma confinement depend on the edge behavior.^{1,2} Remarkably, during recent years experiments have shown that electrostatic turbulence induces anomalous edge particle transport. Nowadays, the intensive research on edge turbulence and transport has been motivated by the unexpected results obtained with large tokamaks.²

As it was originally proposed in the seventies,³ the utilization of external magnetic perturbation is currently used in some tokamak devices to create a chaotic magnetic configuration at the plasma edge. This configuration is adequate to control particle and heat diffusion and, consequently, to improve the plasma confinement. Accordingly, the magnetic field lines at the plasma edge may become chaotic by applying the resonant helical magnetic fields created by external resonant helical windings (RHW),⁴ or ergodic divertors.⁵⁻⁷ The expected effect of these perturbations is to produce uniform particle and heat loads to the wall along chaotic magnetic field lines. The resultant edge cooling reduces impurities, provides screening to impurity influx, and thus improves the confinement characteristics. However, the local effect of these resonant magnetic perturbations on the turbulence and their effect on the transport in the edge remains an open question.^{8,9}

This paper describes an attempt to control the plasma edge turbulence with external electrical currents on the resonant helical windings curled around the TBR (Brazilian Tokamak) tokamak vessel.¹⁰

Other experiments in the TBR tokamak, which employed these resonant field perturbations created by the RHW, were previously done with a field strength lower than

that used in this work⁴ in order to control magnetohydrodynamic (MHD) oscillations¹¹ and turbulence.

In this experiment, external coils have created both magnetic islands and chaotic field regions through island overlapping.¹² Thus, we have studied the influence of the resonances created by the $m=4/n=1$ RHW (m and n determine the poloidal and toroidal wave numbers, respectively) on the plasma edge turbulence.

We needed to measure density, potential temperature fluctuations, and the phases and correlations between these fluctuating quantities^{13,14} for estimating the anomalous particle transport in such turbulent plasma. Thus, we designed and installed at TBR a complex system of probes to simultaneously measure electrostatic and magnetic fluctuations and some plasma mean parameters. To improve the accuracy of these measurements, we have also determined temperature fluctuations and taken them into account to correct density and plasma potential fluctuations.¹⁵

The analysis has shown that the magnetic perturbations reduced the equilibrium parameters and the spectral power of the fluctuations, and enhanced their phase velocity. These perturbations also produced a reduction of the particle flux at the plasma edge. In addition, the bispectral analysis¹⁶⁻²¹ has shown that the RHW suppressed the quadratic coupling, whereas the power functions presented no common specific direction for the energy cascading driven by the fluctuation, i.e., the energy transferred between different spectral components.

The conditions for the existence of intermittency in the measured signals have been investigated with and without the perturbations induced by the RHW. However, no clear evidence of intermittent fluctuations was found, since the departure from a Gaussian distribution, and from a broadband power spectrum with no localized peaks, as well as the small time correlations, was not simultaneously detected for the whole spectrum.

The relation between temperature, potential, and density

^{a)}Electronic mail: ibere@if.usp.br

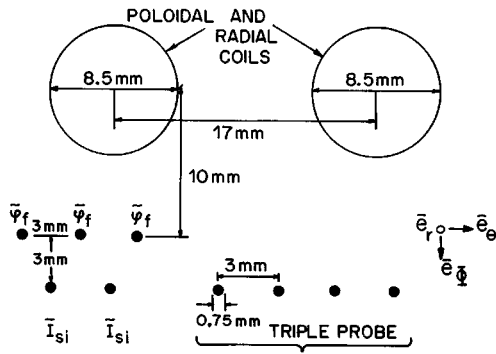


FIG. 1. Scheme of probe assembly.

studied here may contribute to the identification of the basic mechanisms that determine edge turbulence.^{22,23} The correlations between electrostatic and magnetic oscillations have been analyzed and will be published elsewhere.

The outline of this paper is as follows: Section II gives a brief description of the apparatus and basic analysis techniques. In Sec. III we describe the behavior of temperature, density, plasma potential equilibrium, and fluctuation profiles, with and without RHW utilization. In Sec. IV we analyze the spectral and bispectral characteristics of the electrostatic turbulence and the behavior of the anomalous crossfield flux with and without RHW. Section V summarizes the conclusions of this work.

II. APPARATUS AND TECHNIQUES OF ANALYSIS

The experiment was carried out using the ohmically heated TBR tokamak, with major radius $R_o = 0.30$ m, minor radius $a = 0.08$ m, toroidal magnetic field $B = 0.4$ T, plasma current $I_p \approx 10$ kA, chord average density $n_0 \approx 7 \times 10^{18} \text{ m}^{-3}$, and pulse length of 10 ms.¹⁰ The plasma in the TBR has a circular cross section and a full poloidal limiter. We used hydrogen.

The data were collected using a multipin Langmuir probe (see Fig. 1) which was inserted into the plasma through a diagnostic port located at the top of the tokamak, and 45° toroidally displaced from the poloidal limiter.¹⁵ This probe system consisted of four tips, a four-pin probe array and a single-probe tip. Two of the four-pin configuration measured the floating potential fluctuations $\bar{\varphi}_f$, and the other two the ion saturation current fluctuations \bar{I}_{si} . These two pairs of pins were used for determining the spectrum $S(k, f)$, the power weighted average values of poloidal wave vector k_θ , the phase velocity v_{ph} , and the width of k_θ .²⁴ Another single tip, located 3 mm from the four-tip configuration, was used to directly measure the mean value of the floating potential φ_f .

The following quantities were obtained using a modified triple probe technique^{15,25-27} with four pins to correct for phase delay errors: The electron mean temperature T_e , its fluctuation \bar{T}_e , the ion saturation current I_s , and its fluctuation \bar{I}_{si} . Two pairs of magnetic coils were mounted in the same system (Fig. 1) to measure the poloidal, \bar{B}_θ , and the radial, \bar{B}_r , components of the magnetic field fluctuations.

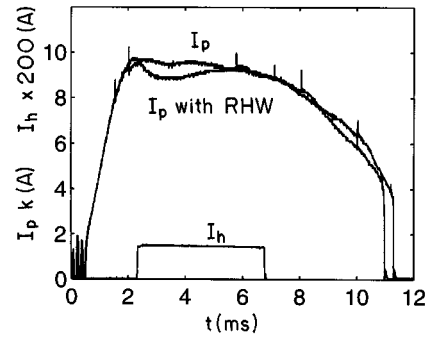


FIG. 2. Time evolution of plasma current (I_p) and RHW current (I_h).

The probe measurements were done during the flattop phase of the plasma current (Fig. 2) in intervals of approximately 4 ms, then they were averaged throughout seven consecutive shots. The time series measurements were recorded using 8 bit digitizers, with a maximum sampling rate of 1 MHz. The data used in the analysis consisted of 105 samples of 256 points. These data were tested with a statistical criterion to discard spurious points that otherwise would have contributed to overestimate the fluctuations.

The plasma density then was obtained by using $n \alpha I_{si} / T_e^{1/2}$. We applied a numerical filter to the data measured by the triple probe in order to separate their mean ($f \leq 5$ kHz) and fluctuating ($5 \text{ kHz} < f < 500 \text{ kHz}$) components.

The density and potential fluctuations, corrected by temperature fluctuations, were obtained using²⁷

$$\bar{n} = n [\bar{I}_{si} / I_{si} - \frac{1}{2} \bar{T}_e / T_e + \frac{1}{8} (\bar{T}_e / T_e)^2] \quad (1)$$

and

$$\bar{\varphi}_p = \bar{\varphi}_f + \sigma K \bar{T}_e / e, \quad (2)$$

where σ is taken as 2.8.¹⁵ The plasma potential (φ_p) is related to the floating potential (φ_f) through an equation similar to Eq. (2).

The external magnetic field perturbation was created by electric currents circulating through a set of helical windings externally located around the torus.²⁸ These coils produced a perturbation field with dominant helicity $m = 4/n = 1$ and average radial amplitude $\langle |B_r(a) / B_\phi| \rangle \approx 0.4\%$ at the limiter radius (B_ϕ is the toroidal equilibrium field, and B_r the radial perturbing field). This perturbation was resonant for an edge safety factor $q \leq 4$. The currents circulating through these coils were set to $I_h = 285$ A, and they were switched on after the plasma current had reached steady values (Fig. 2).

The above-mentioned coils created both magnetic islands and ergodic field regions through island overlapping. Figure 3 shows Poincaré maps computed for those discharges with a natural dominant $m = 2/n = 1$ MHD mode with [Fig. 3(a)] or without [Fig. 3(b)] the effects of resonant perturbations created by the $m = 4/n = 1$ helical windings. To compute these maps, the $m = 2/n = 1$ natural mode (usually observed in the TBR experiments) was described by a current perturbation inside the plasma.¹² In the unperturbed map [Fig. 3(b)] the $m/n = 2/1, 3/1$ and other smaller islands could be recognized. However, the applied field destroyed the

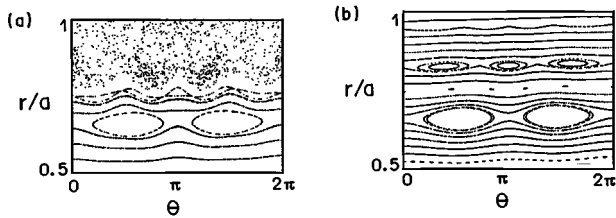


FIG. 3. Poincaré maps showing the poloidal magnetic-field line configurations with RHW (a) or without RHW (b).

magnetic surfaces in an ergodic layer at the plasma edge [Fig. 3(a)] with a radial width of about 1.5×10^{-2} m. This ergodic region did not include the $q=2$ islands and it was created around the unperturbed magnetic surface with the safety factor $q=4$. In this case the stochasticity parameter, computed for $m/n=3/1$ and $m/n=4/1$ island superposition, was $s \approx 1$.¹² Notice that $s = (L_{4/1} + L_{3/1}) / 2(r_{4/1} - r_{3/1})$, where $r_{m/n}$ is the radial coordinate of the magnetic surface with $q(r_{m/n}) = m/n$, and $L_{m/n}$ is the island width at this surface. Thus, in this experiment the RHW created a field line configuration similar to those obtained with ergodic divertors in the tokamak TEXT⁵ (Texas Tokamak) and TORE SUPRA⁷ (Toroidal Supraconducteur-Cadarache).

III. EQUILIBRIUM AND FLUCTUATION PROFILES

A sharp temperature gradient always exists without the RHW utilization [Fig. 4(a)]. With the RHW the radial temperature profile became flat from $r/a=0.81$ to $r/a=0.96$. The existence of this modified flat profile suggests the formation of a layer where the thermal diffusivity is controlled by the chaotic field lines, as was observed in the TORE SUPRA tokamak.^{7,8} The density profile also decreased [Fig. 4(b)] and such behavior has been attributed to the different connection to the walls created by the RHW perturbation, and resulting in a larger area seen by the plasma. Similar alterations were also induced by an ergodic divertor in the TORE SUPRA tokamak.^{7,8}

During RHW operation the floating potential and plasma potential profiles [Figs. 5(a) and 5(b)] were also modified. The utilization of the magnetic perturbation produced a less negative floating potential, in particular near the region $r/a=0.85$, where the effect was clearly seen. This result was also observed in the TEXT tokamak²⁹ for reduced equilibrium parameter discharges.

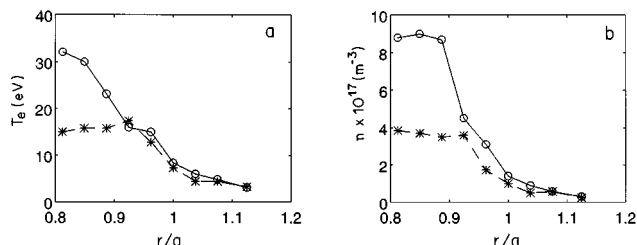


FIG. 4. Radial profiles of electron temperature with (*) or without (O) RHW (a). The same for plasma density profiles (b).

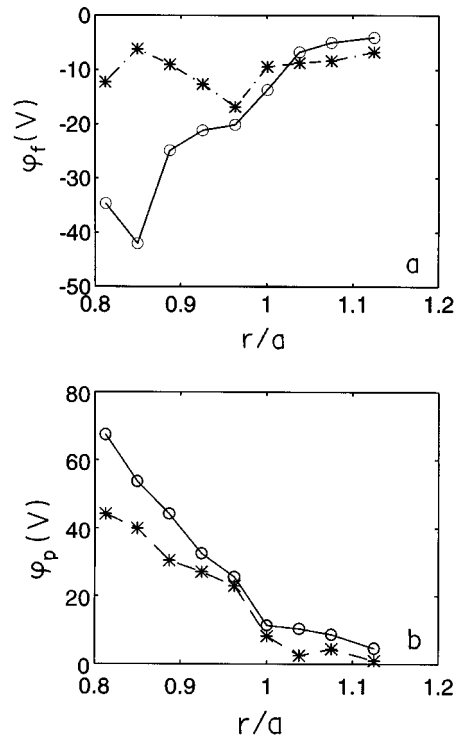


FIG. 5. Radial profiles of floating potential with (*) or without (O) RHW (a). Radial profiles for plasma potential with (*) or without (O) RHW (b).

The radial profile of E_r showed the absence of a shear layer, which was also confirmed by the measured profile of the phase velocity. As has already been mentioned, there is no experimental evidence of the existence of any shear layer in the TBR plasma edge.^{15,28}

The results of this work, when compared with previous measurements,²⁸ show that the changes in the mean parameter profiles (induced by external perturbations) increased with the perturbing field strength.

Figure 6 shows the radial profiles of electron temperature fluctuation (rms) amplitudes normalized to a local mean value, with or without using the RHW. Although the equilibrium and fluctuating temperature were altered by using the RHW, no noticeable effect was detected on the ratio between these two measurements. The same figure also shows the

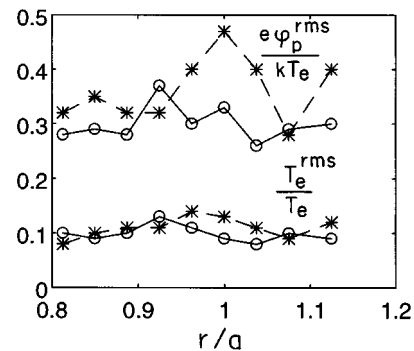


FIG. 6. Edge radial profiles of electron temperature fluctuation rms amplitudes normalized to local mean value of temperature, with (*) or without (O) RHW. The same for the plasma potential.

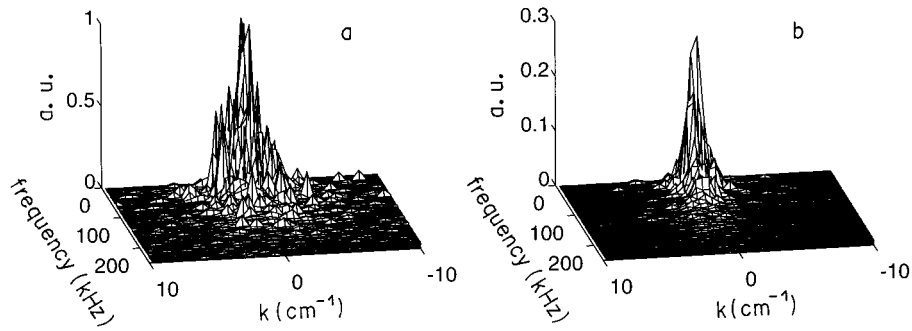


FIG. 7. $S(k, f)$ spectra for density fluctuations at $r/a=0.89$ without RHW (a) or with RHW (b).

normalized plasma potential fluctuation profiles; here a significant alteration may be noticed only at the limiter position.

We observed a steep increase of the mean density value n , and of the plasma potential φ_p , with or without the RHW, in a plasma current scan from 6 to 10 kA, for a constant position $r/a=0.89$ of the probe system. On the other hand, no noticeable alteration was detected in the mean temperature T_e .

IV. ELECTROSTATIC TURBULENCE AND TRANSPORT

To study the effect of RHW on particle transport we investigated the changes in the plasma edge parameters associated with that transport.

Thus we used digital spectral analysis to compute the spectral power density distribution function $S(k, f)$ ²⁴ for fluctuating density and plasma potential. Figure 7 shows the $S(k, f)$ spectra for density fluctuations at the radial position $r/a=0.89$, computed for discharges without magnetic perturbation [Fig. 7(a)], and for perturbed discharges [Fig. 7(b)]. The spectral density functions were strongly decreased by the RHW. These spectra showed that both the wave vector component (k_θ) and its spectral width (σ_{k_θ}) were reduced by using the RHW. This reduction corresponds to a global decrease of the fluctuations and, since the low wave numbers are dominant in the spectrum, it suggests a turbulence stabilization. Although not so well identified, similar alterations were also produced by the RHW on the plasma potential spectra.

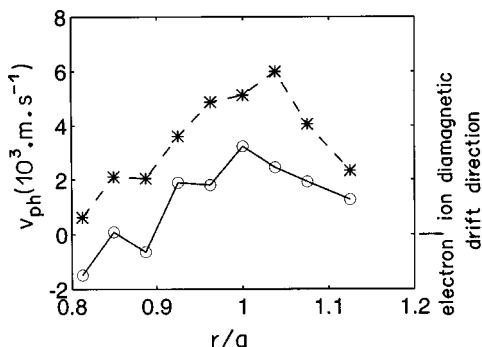


FIG. 8. Phase velocity profiles for plasma potential fluctuations with (*) or without (O) RHW.

Figure 8 shows the phase velocity profiles for plasma potential fluctuations, with or without magnetic perturbations. The poloidal phase velocity inside the plasma has essentially the same direction as the ion diamagnetic drift velocity. The effect of the RHW is to enhance the phase velocity because of the reduction in the average wave vector. The previously reported^{15,28} absence of shear layer has been confirmed in this new experiment.

The driven particle flux Γ , used here is³⁰

$$\Gamma = \frac{2}{B_\phi} \int k_\theta P_{n\varphi} \sin(\theta_{n\varphi}) df. \quad (3)$$

Figure 9 shows particle flux profiles for discharges with or without the RHW perturbation. An appreciable alteration was produced in the plasma edge transport by utilizing resonant perturbations at this field strength. The results show not only a reduction of the particle flux in the whole spectrum but even, for some low frequency intervals, an inversion in its radial direction. This inward transport effect at low frequencies has been associated with drift wave fluctuations driven by ionization effects.^{31,32}

From the radial distribution of electron density at the plasma edge we can roughly estimate the radial diffusion coefficient across the main magnetic field subjected or not to the effect of the applied perturbations. The diffusion coefficient D is given by

$$D = -\Gamma / \nabla n, \quad (4)$$

where Γ is the particle flux. The result that we obtained near the limiter was $D \approx 0.3 \text{ m}^2/\text{s}$. Although the perturbing mag-

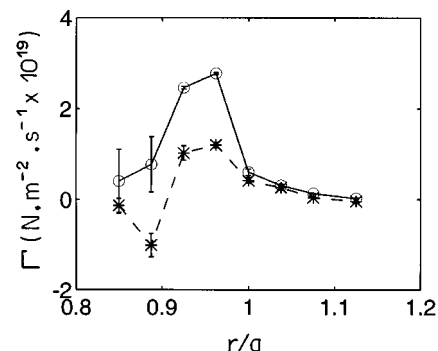


FIG. 9. Induced particle flux profiles with (*) or without (O) RHW.

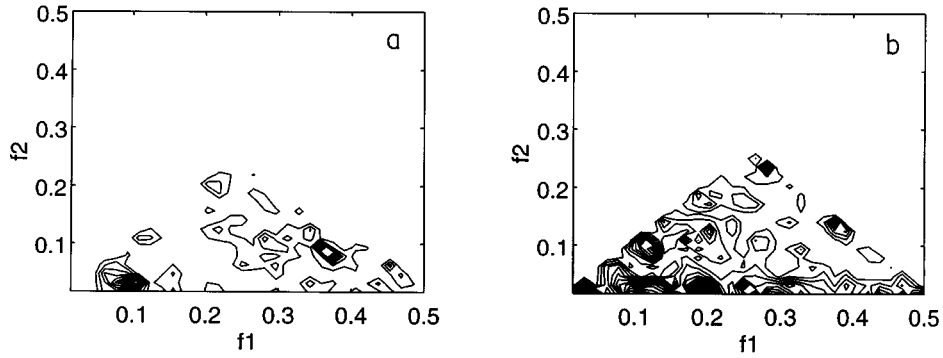


FIG. 10. Bicoherence for ion saturation current fluctuations at $r/a=0.92$ with (a) or without (b) RHW. Data filtered at 250 kHz and frequencies normalized to the Nyquist frequency.

netic field seemed to slightly enhance the diffusion coefficient at the plasma edge, this enhancement falls within the experimental uncertainties.

In order to better understand the experimental results associated with particle transport in the presence of resonance fields, we will compare here the diffusion coefficient, which we have previously computed from our experimental data, with the following theoretically predicted values.⁶ In the collisionless plasma limit with a stochastic field, the diffusion coefficient D^C may be estimated by⁶

$$D^C = \langle D_m \rangle v_{thi}. \quad (5)$$

where D_m , the magnetic diffusion coefficient of the chaotic field lines, is given by

$$D_m = \pi R \langle |Br/B_\phi|^2 \rangle. \quad (6)$$

The ion thermal velocity v_{thi} may be estimated by using the average values of the plasma edge temperatures near the limiter (i.e., $T_i \approx T_e \approx 15$ eV). Thus, we obtained $D^C \approx 0.27$ m²/s for the average radial diffusion coefficient in this region. This value is comparable with that measured experimentally and is thus at variance with the observation that the RHW makes little change to the value of D .

Another formula to calculate D for the collisional low stochasticity limit is⁶

$$D^N = 0.3 \langle Br/B_\phi \rangle \lambda_n c_s, \quad (7)$$

where λ_n is the density scale length, c_s is the ion sound speed, and 0.3 is a factor used to account for similar experimental observations in magnetic limiter⁶ and divertor experiments,³³ as suggested in Ref. 34. For the discharges with RHW, the estimated values of D^N (for the same region considered before) give $D^N \approx 0.05$ m²/s. This diffusion caused by the RHW is small compared with the observed total diffusion. So, the predicted D^N is compatible with our present observation.

A way to investigate the nonlinear coupling among different fluctuation components is to use the bispectral analysis technique, as suggested in Refs. 16 and 19. In the present analysis, however, the recorded data do not have a sufficient number of events for neglecting the variance of the bicoherence (b^2). It has been shown that the variance of bicoherence³⁵ may be estimated by $\sigma_{b^2} \approx 2b/M^{1/2}$ (where $M=210$ is the number of successive realizations with

128 μ s intervals). If we consider the autobicoherence of floating potential, ion saturation current, and temperature fluctuations, then no prominent peaks may be identified. However, a low level of nonlinear coherent interactions (much larger than the statistical uncertainty) was clearly observed in the bispectral analysis, showing that nonlinear coupling exists in electrostatic fluctuations at the edge.

Figure 10 shows the bicoherence of I_{si} fluctuations at $r/a=0.92$, with (a) or without (b) the RHW utilization. The maximum value is $b^2=0.24 \pm 0.03$ for case (a) and $b^2=0.40 \pm 0.05$ for case (b). For the unperturbed oscillations [Fig. 10(b)], nonlinear interactions occur mainly between modes with frequencies $f_2 \leq 50$ kHz and those with $f_1 \leq 120$ kHz. However, the presence of the magnetic perturbations lowered the bicoherence values and reduced the frequency regions to $f_2 \leq 20$ kHz and $f_1 \leq 50$ kHz. A similar situation was observed for the other parameter fluctuations.

Figure 11 shows the integrated bicoherence for the same fluctuations depicted in Fig. 10, with or without resonant fields. The calculated values decreased with the magnetic perturbation. Furthermore, we observed the highest bicoherence values for 50 and 100 kHz components. If we consider any of these two frequency components to satisfy the resonant condition $f=f_1+f_2$, then the bicoherence (for interactions with or without RHW) will not show any contribution from modes of the high frequency band.

We will utilize the method proposed in Refs. 17 and 18

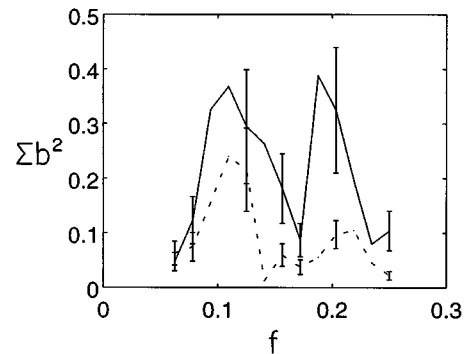


FIG. 11. Integrated bicoherence for ion saturation current fluctuations with (...) or without (—) RHW at $r/a=0.92$. Data were filtered at 250 kHz and frequencies normalized to the Nyquist frequency.

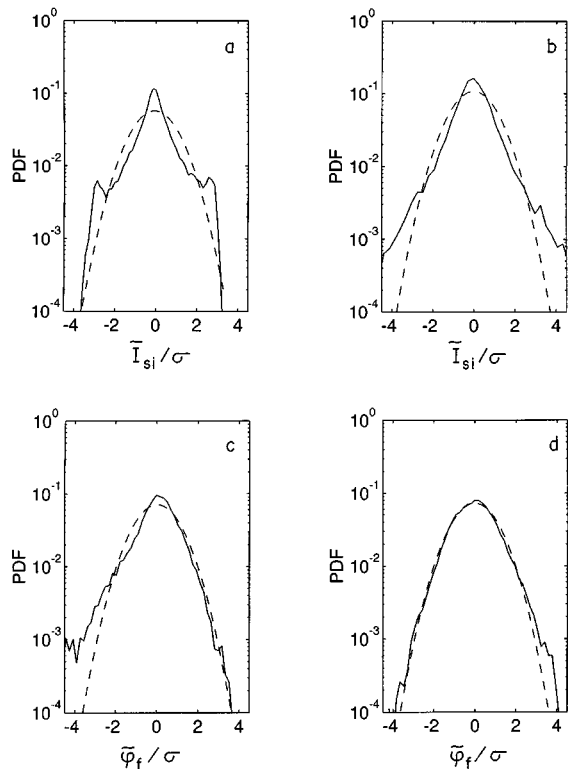


FIG. 12. Probability distribution functions for ion saturation current, without (a) or with (b) RHW, as a function of the fluctuation amplitude normalized to the respective standard deviation. The same for floating potential fluctuations, (c) and (d). The dashed curves represent Gaussians with the same standard deviation.

to evaluate the nonlinear coupling coefficients and the amount of energy cascading between waves. The relationships between fluctuations (monitored at two points in space) are usually described with linear and quadratic transfer functions. From these relationships we can estimate the wave-wave coupling coefficient and the energy transfer between spectral components.¹⁵

The amplitude of the coupling coefficient that gives the strength of coupling between a wave of frequency f and waves of frequencies f_1 and f_2 is not significant, with or without RHW.

The power transfer function shows that the difference-interaction region was dominated by negative transfer rates for floating potential fluctuations. The floating potential fluctuations perturbed by the RHW present a positive power transfer in the difference-interaction region. For ion saturation current fluctuations the power transfer function is much lower than the transfer function of the other parameter fluctuations and presents no preferential direction.

After a data analysis of higher order momenta, such as skewness and kurtosis, we found no clear evidence of Gaussian probability distribution functions for the electrostatic fluctuations with or without the magnetic perturbation. Thus, Fig. 12(a) and 12(b) shows non-Gaussian probability distribution functions obtained for the ion saturation current fluctuations. For these cases the signal has a value almost equal to zero for the skewness, but values significantly different from three for the kurtosis (a Gaussian distribution has a

kurtosis equal to three). The RHW do not alter these distributions. However, for the case shown in Figs. 12(b) and 12(c) for fluctuating potential fluctuations, the magnetic perturbations significantly alter the distribution, which became similar to a Gaussian distribution. Finally, the time correlations are small, nearly $4 \mu\text{s}$, and do not show any change with the RHW.

V. CONCLUSIONS

In this work we present evidences of relevant alterations on the electrostatic spectra and on the turbulence driven transport when the edge magnetic structure became chaotic after the application of external resonant fields.

It should be noted that in TBR not only were the magnetic oscillations strongly reduced, as in other experiments,^{11,36,37} but the electrostatic oscillations were also slightly modified by the resonant helical windings that were used to perturb the magnetic field. The latter effect could be associated with the uncommon (in tokamaks)¹ partially similar frequency spectra for these two kinds of oscillations. In fact, although the electrostatic power spectra present frequencies lower than the Mirnov frequencies, the spectra still show a partial superposition with the magnetic power spectra. Therefore, it may be possible in TBR to routinely alter the magnetic fluctuations in order to control the turbulence spectra at the plasma edge.

Evidence for this kind of control also was recently reported for the reversed field pinches (RFP).^{38,39} However, for tokamaks the magnetic and the electrostatic oscillations do not have the same dominant driven processes, as was suggested for the RFP. In fact, the spectral analysis showed that only a relatively low fraction of the magnetic fluctuation power could be associated with the electrostatic fluctuation power.

Other examples of this influence are the modulation of the electrostatic turbulence by a dominant MHD mode, and the correlations between the magnetic turbulence and the electrostatic transport.⁴⁰

A strong decrease of the measured equilibrium parameter profiles in TBR was observed with the utilization of the RHW. With the magnetic perturbation the temperature profile became flat, which suggests the formation of a layer where the thermal diffusivity would be controlled by the chaotic field lines.⁸ This profile might produce modifications in the density gradient of the plasma current, and allow a possible suppression or stabilization of the internal resistive modes.^{36,41-43} Consequently, this effect might contribute to the observed decrease in the turbulence fluctuation at the plasma edge. The density profile also decreased in discharges perturbed by the RHW, since the chaotic field line diffusion to the walls had increased.⁴⁴

In addition to the mentioned alterations of the mean and the fluctuating values, the ratios between these quantities, or more specifically, the level of density (n_e^{rms}/n_e), temperature (T_e^{rms}/T_e) and potential ($e\varphi_p^{\text{rms}}/kT_e$) remained approximately constant when the resonant field was activated.

The radial profile of the plasma potential was lowered and smoothed by the perturbation, consequently, the radial

electric field E_r decreased monotonically. This radial variation of E_r reinforces the previous measurements²⁸ that show the absence of a shear layer in the TBR discharges.

The alterations on the spectral power distributions due to the RHW perturbation suggest a global decrease of the turbulence level.

The phase velocities of electrostatic fluctuations inside the plasma are essentially in the direction of the ion diamagnetic drift velocity. The effect of the RHW perturbation is to enhance the phase velocity because of the reduction of the average wave vector.

The effect of external perturbations is to enhance the linear correlation between the electrostatic fluctuations.

The use of the RHW also produces a significant alteration on the particle flux profiles at the plasma edge. The particle flux shows not only a reduction but, even for some low frequency components, an inversion in its radial direction. However, this inward transport produces only a small overall effect on the frequency integrated transport. Theoretical studies show that the drift wave fluctuations driven by ionization effect could have generated the observed inward transport.³¹

The particle diffusion coefficients, calculated from the particle flux and density edge gradient for discharges with or without RHW, showed no significant differences. The coefficient computed by considering the randomization of the field lines gives a value compatible with our experimental results.

We used bispectral analysis to investigate nonlinear coupling. Although the autobicoherences of electrostatic fluctuations showed no prominent peaks, a low level of nonlinear coupling was clearly observed. The effect of the magnetic perturbations was to reduce these bicoherences for all measured oscillations.

The power transfer function shows that for floating potential fluctuations the transfer of energy occurs in the negative direction, i.e., from high to low frequency modes. The RHW reverses this direction. For ion saturation current fluctuations the power transfer functions are much lower than floating potential transfer functions and present no preferential direction.

Data analyses of higher order momenta, such as skewness and kurtosis, with or without the magnetic perturbation, revealed no clear evidence of Gaussian probability distribution functions.

This analysis is not conclusive regarding the existence of intermittency in the fluctuating parameters measured at the TBR plasma edge for the discharges with or without RHW. The small time correlation and high values for the kurtosis suggest the existence of intermittency in the data, but since the measured fluctuating parameters exhibited some significant peaks in their autospectra, we believe there is not enough evidence for such a conclusion. To confirm the existence of the intermittency, we are doing a more detailed analysis using correlation and conditional averaging techniques.⁴⁵

ACKNOWLEDGMENTS

The authors would like to thank Dr. F. Karger, Dr. D. Biskamp (Max-Planck-Institut für Plasma Physik, Germany), Dr. R. D. Bengtson, and Dr. S. McCool (Fusion Research Center, The University of Texas at Austin, USA) for many fruitful discussions. The authors are also thankful to Dr. Edgardo Browne (Lawrence Berkeley Laboratory) for revising the manuscript, Gisele Oda, for computing the Poincaré maps shown in this work, and to Dr. A. N. Fagundes and W. P. Sá (University of São Paulo, Brazil), for their computational assistance.

This work was partially supported by the Brazilian research agencies FAPESP and CNPq.

- ¹A. J. Wootton, B. A. Carreras, H. Matsumoto, K. McGuire, W. A. Peebles, Ch. P. Ritz, P. W. Terry, and S. J. Zweben, *Phys. Fluids B* **2**, 2879 (1990).
- ²F. Wagner and U. Stroth, *Plasma Phys. Controlled Fusion* **35**, 1321 (1993).
- ³F. Karger and K. Lackner, *Phys. Lett. A* **61**, 385 (1978).
- ⁴R. M. Castro, M. V. A. P. Heller, I. L. Caldas, R. P. da Silva, and Z. A. Brasílio, *Nuovo Cimento (D)* **15**, 983 (1993).
- ⁵S. C. McCool, A. J. Wootton, A. Y. Aydemir, R. D. Bengtson, J. A. Oedo, R. V. Bravenec, D. L. Brower, J. S. DeGrassie, T. E. Evans, S. P. Fan, J. C. Forster, M. S. Foster, K. W. Gentle, M. Kotschenreuther, N. C. Luhmann, Jr., W. H. Miner, Jr., T. L. Rhodes, B. Richards, Ch. P. Ritz, D. W. Ross, W. L. Rowan, P. M. Schoch, B. O. Smith, J. C. Wiley, X. H. Yu, and S. B. Zheng, *Nucl. Fusion* **29**, 547 (1989).
- ⁶S. C. McCool, A. J. Wootton, M. Kotschenreuther, A. Y. Aydemir, R. V. Bravenec, J. S. DeGrassie, T. E. Evans, R. L. Hickok, B. Richards, W. L. Rowan, and P. M. Schoch, *Nucl. Fusion* **30**, 167 (1990).
- ⁷A. Grosman, P. Gendrih, C. DeMichelis, P. Mourier-Garbet, J. C. Vallet, H. Capes, M. Chatelier, T. E. Evans, A. Géraud, M. Goniche, C. Grisolia, D. Guilhem, G. Harris, W. Hess, F. Nguyen, L. Poutchy, and A. Samain, *J. Nucl. Mat.* **196**, 59 (1992).
- ⁸J. Payan, X. Garbet, J. H. Chatenet, F. Clairet, C. De Michelis, P. Devynck, P. Ghendrih, C. Gil, A. Grosman, R. Guirlet, W. Hess, J. Lassalle, C. Laviro, M. Paume, A. Truc, P. Hennequin, F. Gervais, and A. Quemeneur, *Nucl. Fusion* **35**, 1357 (1995).
- ⁹T. C. Hender, R. Fitzpatrick, A. W. Morris, P. G. Carolan, R. D. Durst, T. Edlington, J. Ferreira, S. J. Fielding, P. S. Haynes, J. Hugill, I. J. Jenkins, R. J. La Haye, B. J. Parham, D. C. Robinson, T. N. Todd, M. Valovic, and G. Vayakis, *Nucl. Fusion* **32**, 2091 (1992).
- ¹⁰I. C. Nascimento, I. L. Caldas, and R. M. O. Galvão, *J. Fusion Energy* **12**, 295 (1993).
- ¹¹A. Vannucci, O. W. Bender, I. L. Caldas, I. H. Tan, I. C. Nascimento, and E. K. Sanada, *Nuovo Cimento D* **10**, 1193 (1989).
- ¹²A. S. Fernandes, M. V. A. P. Heller, I. L. Caldas, *Plasma Phys. Controlled Fusion* **30**, 1203 (1988).
- ¹³W. Horton, *Phys. Rep.* **192**, 1 (1990).
- ¹⁴J. D. Callen, *Phys. Fluids B* **4**, 2142 (1992).
- ¹⁵R. M. Castro, M. V. A. P. Heller, I. L. Caldas, R. P. da Silva, Z. A. Brasílio, and I. C. Nascimento, *Phys. Plasmas* **3**, 971 (1996).
- ¹⁶Y. J. Kim and E. J. Powers, *IEEE Trans. Plasma Sci.* **PS-7**, 120 (1979).
- ¹⁷Ch. P. Ritz and E. J. Powers, *Physica D* **20**, 320 (1986).
- ¹⁸Ch. P. Ritz, E. J. Powers, and R. D. Bengtson, *Phys. Fluids B* **1**, 153 (1989).
- ¹⁹K. Rypdal and F. Øynes, *Phys. Lett. A* **184**, 114 (1993).
- ²⁰T. Estrada, E. Sanches, C. Hidalgo, B. Brañas, and Ch. P. Ritz, *Proceedings of the 20th EPS Conference on Controlled Fusion and Plasma Physics*, Lisbon, 1993, *Europhysics Conference Abstracts (European Physical Society, Petit-Lancy, 1994)*, Vol. 17C, Part 1, p. 373.
- ²¹H. Y. Tsui, K. Rypdal, Ch. P. Ritz, and A. J. Wootton, *Phys. Rev. Lett.* **70**, 2565 (1993).
- ²²D. Biskamp, *Nonlinear Magnetohydrodynamics* (Cambridge University Press, Cambridge, 1993).
- ²³S. J. Camargo and H. Tasso, *Phys. Fluids B* **4**, 1199 (1992).
- ²⁴S. J. Levinson, J. M. Beall, E. J. Powers, and R. D. Bengtson, *Nucl. Fusion* **24**, 527 (1984).
- ²⁵H. Ji, H. Toyama, K. Yamagishi, S. Shinohara, A. Fujisawa, and K. Miyamoto, *Rev. Sci. Instrum.* **62**, 2326 (1991).

- ²⁶H. Ji, H. Toyama, K. Miyamoto, S. Shinohara, and A. Fujisawa, *Phys. Rev. Lett.* **67**, 62 (1991).
- ²⁷H. Y. Tsui, R. D. Bengtson, G. X. Li, H. Lin, M. Meier, Ch. P. Ritz, and A. J. Wootton, *Rev. Sci. Instrum.* **63**, 4608 (1992).
- ²⁸M. V. A. P. Heller, R. M. Castro, Z. A. Brasilio, I. L. Caldas, and R. P. da Silva, *Nucl. Fusion* **35**, 59 (1995).
- ²⁹X. Z. Yang, B. Z. Zhang, A. J. Wootton, P. M. Schoch, B. Richards, D. Baldwin, D. L. Brower, G. G. Castle, R. D. Hazeltine, J. W. Heard, R. L. Hickok, W. L. Li, H. Lin, S. C. McCool, V. J. Simcic, Ch. P. Ritz, and C. W. Yu, *Phys. Fluids B* **3**, 3448 (1991).
- ³⁰T. L. Rhodes, C. P. Ritz, and R. D. Bengtson, *Nucl. Fusion* **33**, 1147 (1993).
- ³¹A. S. Ware, P. H. Diamond, H. Bigliari, B. A. Carreras, L. A. Charlton, J. N. Leboeuf, and A. J. Wootton, *Phys. Fluids B* **4**, 877 (1992).
- ³²S. Raychoudhury and P. K. Kaw, *Phys. Fluids B* **1**, 1646 (1989).
- ³³A. Nicolai, F. Schöngen, and D. Reiter, *Plasma Phys.* **27**, 1479 (1985).
- ³⁴S. J. Fielding and A. J. Wootton, *Phys. Scr.* **23**, 97 (1981).
- ³⁵Ph. van Milligen, C. Hidalgo, and E. Sanchez, *Phys. Rev. Lett.* **74**, 395 (1995).
- ³⁶Pulsator Team, *Nucl. Fusion* **25**, 1059 (1985).
- ³⁷C. Robinson, *Nucl. Fusion* **25**, 1101 (1985).
- ³⁸J. S. Sarff, S. A. Hokin, H. Ji, S. C. Prager, and C. R. Sovinec, *Phys. Rev. Lett.* **73**, 3670 (1994).
- ³⁹G. Li, J. R. Drake, H. Bergsaker, J. H. Brzozowski, G. Hellblom, S. Mazur, A. Möller, and P. Nordlund, *Phys. Plasmas* **2**, 2615 (1995).
- ⁴⁰N. Ohyaabu, G. L. Jahns, R. D. Stambaugh, and E. J. Strait, *Phys. Rev. Lett.* **58**, 120 (1987).
- ⁴¹H. Tasso, *Plasma Phys.* **17**, 1131 (1975).
- ⁴²M. F. F. Nave, A. W. Edwards, K. Hirsch, M. Hugon, A. Jacchia, E. Lazzaro, H. Salzmänn, and P. Smeulders, *Nucl. Fusion* **32**, 825 (1992).
- ⁴³A. Tomimura, R. M. O. Galvão, *Nucl. Fusion* **33**, 1089 (1993).
- ⁴⁴M. V. A. P. Heller and I. L. Caldas, *Nuovo Cimento D* **14**, 695 (1992).
- ⁴⁵A. V. Filippas, R. D. Bengtson, G. X. Li, M. Meier, Ch. P. Ritz, and E. J. Powers, *Phys. Plasmas* **2**, 839 (1995).